Low Peak-to-Average-Power-Ratio Filter Design

Mahmoud Alizadeh

Department of Electrical and Information Technology
Lund University

Advisor: Thomas Magesacher

March 22, 2013

Printed in Sweden
E-huset, Lund, 2013

Abstract

High Peak-to-Average-Power Ratio (PAPR) is one of the main problems of Multi-Carrier Modulation (MCM) systems. A number of different methods are proposed to reduce the PAPR. Since filtering is often a part of the processing chain in communication systems, PAPR can regrow.

This thesis investigates ways to design peak-aware filters. Filter design with minimum l_1-norm is the approach of the thesis to reach a lower PAPR. Three different methods are investigated, the first one is filter design using spectral factorization. Convex optimization is used as a powerful tool for the other two methods which are least squares filter and equiripple filter designs.

The results show that the minimum l_1-norm filters constructed by the spectral factorization method usually have better performance than their corresponding minimum-phase versions in terms of PAPR gain. For least squares filter and equiripple filter designs using convex optimization, it is possible to achieve a gain in PAPR by accepting extra errors in the frequency response of filters.

Acknowledgements

First of all, I would like to express the deepest gratitude to my supervisor Dr. Thomas Magesacher for his kindly helps, patient guidances and motivations during my master thesis work. His several important feedbacks and suggestions on the thesis report also enhanced it as well.

In addition, I am very grateful to my examiner Dr. Stefan Höst for his precious comments and advices on the report and thesis work in order to have a better performance.

Finally, I would like to thank my parents for their love and all friends that supported me.

Mahmoud Alizadeh
Lund University

Table of Contents

1 Introduction **9**
- 1.1 Overview . . . 9
- 1.2 Problem of MCM Systems . . . 9
- 1.3 Previous Work . . . 9
- 1.4 Goals and Scope . . . 10
- 1.5 Structure of the Thesis . . . 10

2 Peak-to-Average-Power Ratio **11**
- 2.1 Definition of Instantaneous PAPR . . . 11
- 2.2 The CCDF Criterion . . . 13
- 2.3 PAPR Reduction Techniques . . . 19

3 l_1-Norm and Spectral Factorization Method **21**
- 3.1 l_1-Norm Definition . . . 21
- 3.2 Autocorrelation Function and Spectral Factorization Method . . . 22
- 3.3 Minimum l_1-Norm Filter . . . 24

4 Filter Design Using Convex Optimization **31**
- 4.1 Convex Theory . . . 31
- 4.2 Filter Design . . . 33

5 Comparisons **41**

6 Conclusions and Further Work **47**
- 6.1 Summary and Conclusions . . . 47
- 6.2 Further Work . . . 47

References **49**

List of Figures

2.1 A typical block diagram of an OFDM system 12
2.2 PAPR versus the number of subcarriers 12
2.3 Three distributions of input sequence 13
2.4 Differential entropy versus peak power 16
2.5 The PDF of the sum of two independent random variables 17
2.6 The PDF of X and $Y = X^2$ 19
2.7 An exemplary linear phase FIR filter 19
2.8 The CCDF of PAPR of the input and output sequences 20

3.1 The roots of an exemplary autocorrelation function 23
3.2 The roots of autocorrelation function and a group of N-roots 25
3.3 The roots of the minimum l_1-norm filter 26
3.4 The frequency response of the given minimum phase filter 27
3.5 The output CCDF of PAPR of filters 27
3.6 The roots of an exemplary given least squares filter 28
3.7 An example of minimum l_1-norm filter with no PAPR gain 29
3.8 The frequency response of the give least squares filter 29

4.1 Convex and non-convex sets 31
4.2 An example of convex function 32
4.3 Sum of squared error of the filters versus time delays (T) 35
4.4 The output CCDF of PAPR of the LS filters with a relaxation 36
4.5 The frequency responses of the least squares filters with a relaxation 37
4.6 The output CCDF of PAPR of the equiripple filters with a thresholds 40
4.7 The frequency responses of the equiripple filters with a thresholds . . 40

5.1 The output CCDF of PAPR of the three different filters [example 1] . 42
5.2 The frequency response of the three different filters [example 1] . . . 42
5.3 The output CCDF of PAPR of the three different filters [example 2] . 43
5.4 The frequency response of the three different filters [example 2] . . . 44
5.5 The output CCDF of PAPR of the three different filters [example 3] . 45
5.6 The frequency response of the three different filters [example 3] . . . 45

List of Tables

4.1 Least squares filters with a relaxation 37
4.2 Equiripple filters with different l_1-norm constraints 39

5.1 The comparison of three filter design methods 43

List of Acronyms

MCM Multi-Carrier Modulation

DAB Digital Audio Broadcasting

DVB-T Digital Video Broadcasting-Terrestrial

DSL Digital Subscriber Line

OFDM Orthogonal Frequency Division Multiplexing

PAPR Peak-to-Average-Power Ratio

CCDF Complementary Cumulative Distribution Function

PDF Probability Density Function

PMF Probability Mass Function

BER Bit-Error Rate

PSD Power Spectral Density

FIR Finite Impulse Response

WSS Wide Sense Stationary

1 Introduction

1.1 Overview

Multi-Carrier Modulation (MCM) is an elegant modulation scheme in communication systems and is used in many systems such as Digital Audio Broadcasting (DAB), Digital Video Broadcasting-Terrestrial (DVB-T), Digital Subscriber Line (DSL), the IEEE 802.11 (WiFi) and IEEE 802.16 (WiMAX) standards. Orthogonal Frequency Division Multiplexing (OFDM) is a sophisticated type of MCM, which is robust to frequency selective channels, has high bandwidth efficiency, and can be implemented at comparably low cost [1].

1.2 Problem of MCM Systems

Although MCM has established itself in many communication systems, it is still suffering from some problems: PAPR is one of the major problems. Each OFDM symbol is a linear combination of the input symbols. Depending on the symbols' values, the corresponding subcarrier waveforms may align such that their sum has a very large absolute value at one or more points in time and thus results in peaks. As a consequence the Peak-to-Average-Power Ratio (PAPR) becomes high. In order to tolerate the peakiness, an amplifier with high dynamic range is required, which reduces the power efficiency [1].

1.3 Previous Work

There are several classes of methods to reduce the PAPR [2], [3], such as clipping and noise shaping, tone reservation, active constellation extension, tone injection, etc. Each of these methods has some advantages and disadvantages. Clipping is the simplest way to mitigate PAPR, but it is a non-linear process causing signal distortion and out-of-band spectral radiation [1]. PAPR regrowth may occur after using an interpolation filter [4]. In fact a filter may regrow the PAPR, which motivates the design of a filter that leads to lower PAPR. In [4] and [13], minimum l_1-norm filter design has been introduced as an approach to reduce the PAPR. The proposed method in [13] tried to solve the problem for the special case when the magnitude and phase of the transfer function is given.

1.4 Goals and Scope

In this thesis, three methods are investigated in order to design minimum l_1-norm filters. The first one uses the spectral factorization method and is a continuation of the work in [4]. The idea behind this method is the following: for a filter with given magnitude response, all spectral factors can be constructed by forming combinations of autocorrelation roots which are not conjugate reciprocal. This leads to filters with different coefficients but same magnitude response. Least squares filter design is the second method which uses convex optimization to minimize l_1-norm subject to a maximum error of the filter's frequency response. And the last method is equiripple filter design which uses convex optimization to minimize the frequency error of the filter subject to an l_1-norm constraint.

1.5 Structure of the Thesis

The definition of PAPR and problems of high PAPR are described in Chapter 2. Since the simulation is limited by the length of the input sequence, an analytical way is introduced to compute the Complementary Cumulative Distribution Function (CCDF) of PAPR.

In Chapter 3 the definition of the l_1-norm is explained and a short proof showing how this property of a filter determines the support of the output sequences is presented. Furthermore, in this chapter the spectral factorization method is used to construct all filters with the same autocorrelation function and to find the best filter in terms of minimum l_1-norm.

Least squares filter and equiripple filter designs using convex optimization are described in Chapter 4.

Evaluations and comparisons between three filter design methods are explained in Chapter 5.

Finally, in Chapter 6, conclusions and suggestions for further work are summarized.

2

Peak-to-Average-Power Ratio

The Peak-to-Average-Power Ratio (PAPR) is an important issue of communication systems, especially in Multi-Carrier Modulation (MCM) systems. With increasing number of subcarriers, the PAPR levels grow.

High PAPR levels cause several problems [2] and are thus undesirable. It requires power amplifiers with larger dynamic range which are more costly and cause a higher power consumption. Increasing Bit-Error Rate (BER) and out-of-band spectral radiation are other consequences of high PAPR.

This chapter describes the definition of PAPR, and also explains how to compute its CCDF analytically, which is one of the criteria to measure the performance of PAPR reduction techniques.

2.1 Definition of Instantaneous PAPR

For a sequence of complex-valued time-domain transmit data samples $s[n], n = 0, ..., N-1$, which can be a sequence of an OFDM block, the PAPR is defined as [7]

$$\mathrm{PAPR} = \frac{\max\limits_{n} |s[n]|^2}{\frac{1}{N}\sum\limits_{n=0}^{N-1} |s[n]|^2} \tag{2.1}$$

In an OFDM system (a simple block diagram is shown in Figure 2.1), each OFDM symbol is generated by taking an inverse Fourier transform of data symbols $x[k]$

$$s[n] = \sum_{k=0}^{N-1} x[k] e^{j2\pi \frac{k}{N} n} \tag{2.2}$$

High peak amplitudes can appear when the length of the block increases, i.e. for a block consisting of N sinusoidal signals, peaks can arise when many sinusoidal signals align due to their phases such that one or more large peaks arise. This problem becomes worse as N rises since there are more sinusoidal signals whose peaks can align [7].

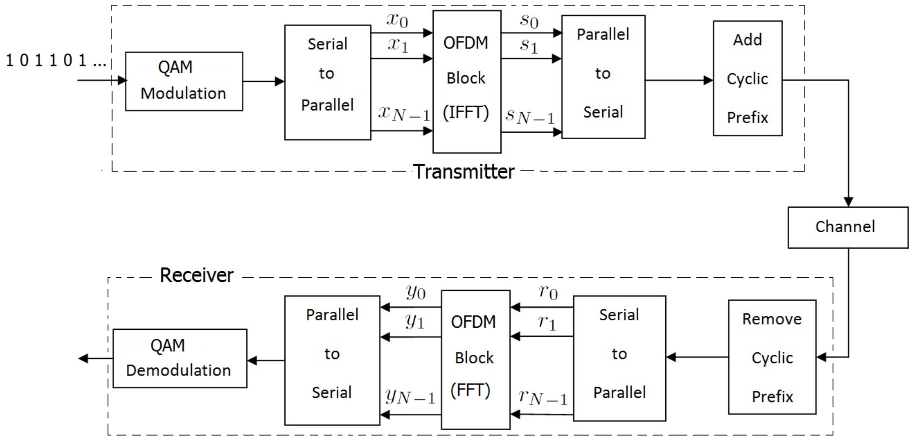

Figure 2.1: A typical block diagram of an OFDM system

Figure 2.2 depicts the relation between the PAPR level for probability 10^{-3} and the number of subcarriers for an OFDM system where all subcarriers are modulated with 4-QAM.

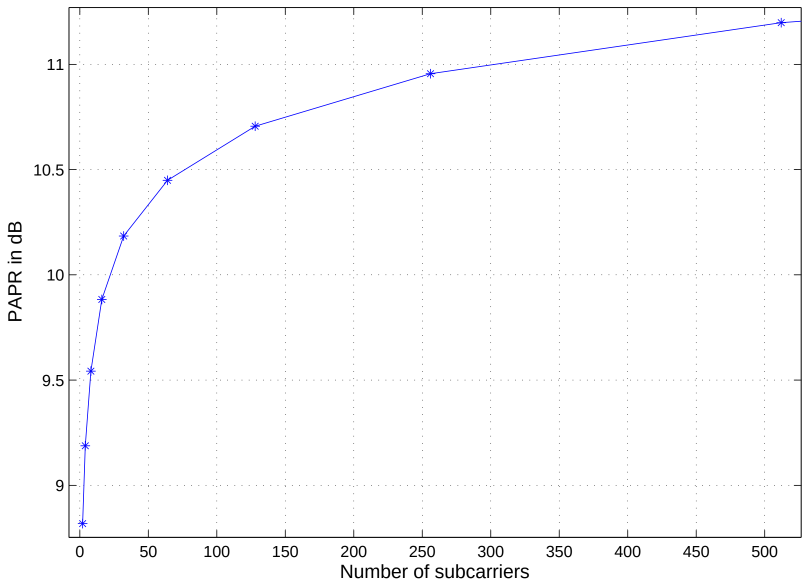

Figure 2.2: PAPR in dB for probability 10^{-3} versus the number of subcarriers in an OFDM system (4-QAM constellation for all subcarriers)

2.2 The CCDF Criterion

In order to measure the performance of PAPR reduction methods, the Complementary Cumulative Distribution Function (CCDF) of PAPR has been introduced as a criterion.

2.2.1 Definition

The CCDF of PAPR is defined as the probability that the instantaneous PAPR exceeds a certain level [7]

$$P(\mathrm{PAPR} > \mathit{level}) \tag{2.3}$$

In the following sections the CCDF of PAPR is calculated for different types of distributions of data sequences analytically.

2.2.2 Input Distributions

In this thesis, three types of distributions of transmit signals are considered: uniform, Gaussian and truncated Gaussian. Figure 2.3 shows the Probability Density Function (PDF) of the three distributions: the uniform distribution sequence is on the interval $[-1, +1]$, the Gaussian PDF is zero mean with the variance $\sigma^2 = 1$, and finally the truncated Gaussian PDF has a Gaussian like distribution but limited on the interval $[-1, +1]$.

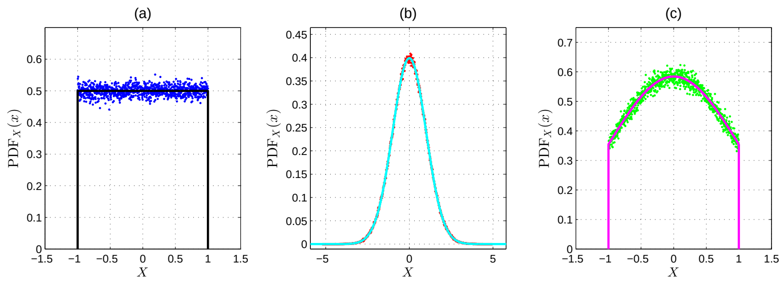

Figure 2.3: Three distributions of input sequence, (a) uniform PDF, (b) Gaussian PDF and (c) truncated Gaussian PDF; dotted lines (.) are the simulation PDF and solid lines (-) are the analytical PDF

For the evaluation of peakiness of the signal and differential entropy the following parameters are of interest:

- peak-to-average-power ratio
- peak-power-to-differential-entropy ratio
- average-power-to-differential-entropy ratio

The average power of a random variable X on the interval $[-a, +a]$ is

$$P_{\mathrm{av}}(X) = E\{X^2\} = \int_{-a}^{+a} x^2 f_X(x)\mathrm{d}x \tag{2.4}$$

where $f_X(x)$ is the PDF of X.

In information theory, the entropy is a measure for the uncertainty of a random variable. For a continuous random variable the differential entropy is defined as

$$H(X) = -\int\limits_{R} f_X\,(x) \log_2 f_X\,(x)\;\mathrm{d}x \tag{2.5}$$

where R is the interval of the distribution and the base of the logarithm is here chosen to be 2 which yields results measured in bits. For a discrete random variable X which can take possible values $\{x_1,\, x_2,\, \ldots,\, x_N\}$ with the Probability Mass Function (PMF) $p(x)$, the entropy is

$$H(X) = -\sum_{i=1}^{N} p\,(x_i) \log_2 p\,(x_i) \tag{2.6}$$

Uniform Distribution

For the continuous random variable X with uniform distribution on the interval $R = [-a,\, +a]$ and $f_X(x) = \frac{1}{2a}$, the average power or variance can be computed as

$$P_{\mathrm{av}}(X) = E\{\,X^2\} \;= \int_{-a}^{a} x^2\,\frac{1}{2a}\,\mathrm{d}x = \frac{a^2}{3} \tag{2.7}$$

Thus, the peak-to-average-power ratio of the uniform distribution is

$$PAPR = \frac{a^2}{\left(\frac{a^2}{3}\right)} = 3 \tag{2.8}$$

and the differential entropy is

$$H(X) = -\int\limits_{-a}^{a} \frac{1}{2a} \log_2\left(\frac{1}{2a}\right) \mathrm{d}x = \log_2(2a) \tag{2.9}$$

Then, the average-power-to-differential-entropy ratio can be obtained as

$$\frac{P_{\mathrm{av}}(X)}{H(X)} = \frac{a^2}{3\,\log_2(2a)} = \frac{\sigma_x^2}{\log_2\left(\sigma_x\sqrt{12}\right)} \tag{2.10}$$

and the peak-power-to-differential-entropy ratio is

$$\frac{P_{\mathrm{peak}}(X)}{H(X)} = \frac{a^2}{\log_2(2a)} = \frac{3\,\sigma_x^2}{\log_2\left(\sigma_x\sqrt{12}\right)} \tag{2.11}$$

Gaussian Distribution

Gaussian distribution with a variance σ_x^2 has infinite support. Although infinite values never occur in practice, the Gaussian distribution is commonly used to model signals and noise [4].

The differential entropy of the Gaussian distribution is

$$H(X) = -\int_{-\infty}^{+\infty} \frac{1}{\sigma_x\sqrt{2\pi}} e^{-\frac{x^2}{2\sigma_x^2}} \log_2\left(\frac{1}{\sigma_x\sqrt{2\pi}} e^{-\frac{x^2}{2\sigma_x^2}}\right) \mathrm{d}x = \frac{\ln\left(2\pi e \sigma_x^2\right)}{2\ln(2)} \tag{2.12}$$

Truncated Gaussian Distribution

The probability density of truncated Gaussian function is similar to Gaussian distribution but limited to the support $[-a, +a]$, and its PDF is given by

$$f_{X_{tG}}(x) = \frac{f_{X_G}(x)}{\mathrm{erf}\left(\frac{a}{\sqrt{2}\,\sigma_x}\right)} \tag{2.13}$$

where $f_{X_G}(x)$ is the Gaussian PDF. The denominator is the normalization term corresponding to the area of the Gaussian PDF on the interval $[-a, +a]$

$$\int_{-a}^{+a} f_{X_G}(x)\,\mathrm{d}x = \int_{-a}^{+a} \frac{1}{\sigma_x\sqrt{2\pi}}\, e^{-\frac{x^2}{2\sigma_x^2}}\,\mathrm{d}x = \mathrm{erf}\left(\frac{a}{\sqrt{2}\,\sigma_x}\right) \tag{2.14}$$

In the following the average power of the truncated Gaussian PDF is calculated

$$\begin{aligned} E\{X^2\} &= \int_{-a}^{+a} x^2 f_{X_{tG}}(x)\,\mathrm{d}x = \\ &\int_{-a}^{+a} x^2 \frac{1}{\sigma_x\sqrt{2\pi}} \frac{e^{-\frac{x^2}{2\sigma_x^2}}}{\mathrm{erf}\left(\frac{a}{\sqrt{2}\,\sigma_x}\right)}\,\mathrm{d}x = \sigma_x^2 - \frac{a\sqrt{2}\,\sigma_x\, e^{-\frac{a^2}{2\sigma_x^2}}}{\sqrt{\pi}\,\mathrm{erf}\left(\frac{a}{\sqrt{2}\,\sigma_x}\right)} = \\ &\sigma_x^2 \left(1 - \frac{2\,a\,e^{-\frac{a^2}{2\sigma_x^2}}}{\sigma_x\sqrt{2\,\pi}\,\mathrm{erf}\left(\frac{a}{\sqrt{2}\,\sigma_x}\right)}\right) \end{aligned} \tag{2.15}$$

The differential entropy of the truncated Gaussian distribution is

$$\begin{aligned} H(X) = -\int_{-\infty}^{+\infty} &\frac{1}{\sigma_x\sqrt{2\pi}\,\mathrm{erf}\left(\frac{a}{\sqrt{2}\,\sigma_x}\right)} e^{-\frac{x^2}{2\sigma_x^2}} \log_2\left(\frac{1}{\sigma_x\sqrt{2\pi}\,\mathrm{erf}\left(\frac{a}{\sqrt{2}\,\sigma_x}\right)} e^{-\frac{x^2}{2\sigma_x^2}}\right) \mathrm{d}x = \\ &\frac{2\ln\left(\sigma_x\sqrt{2\pi}\ \mathrm{erf}\left(\frac{a}{\sqrt{2}\,\sigma_x}\right)\right)+1}{2\ln(2)} - \frac{a}{\ln(2)\sigma_x\sqrt{2\pi}\,\mathrm{erf}\left(\frac{a}{\sqrt{2}\,\sigma_x}\right)} e^{-\frac{a^2}{2\sigma_x^2}} \end{aligned} \tag{2.16}$$

Figure 2.4 shows differential entropy versus peak power for the three distributions (when the variance is one). It is clear that the uniform distribution has minimum entropy and Gaussian distribution has highest entropy.

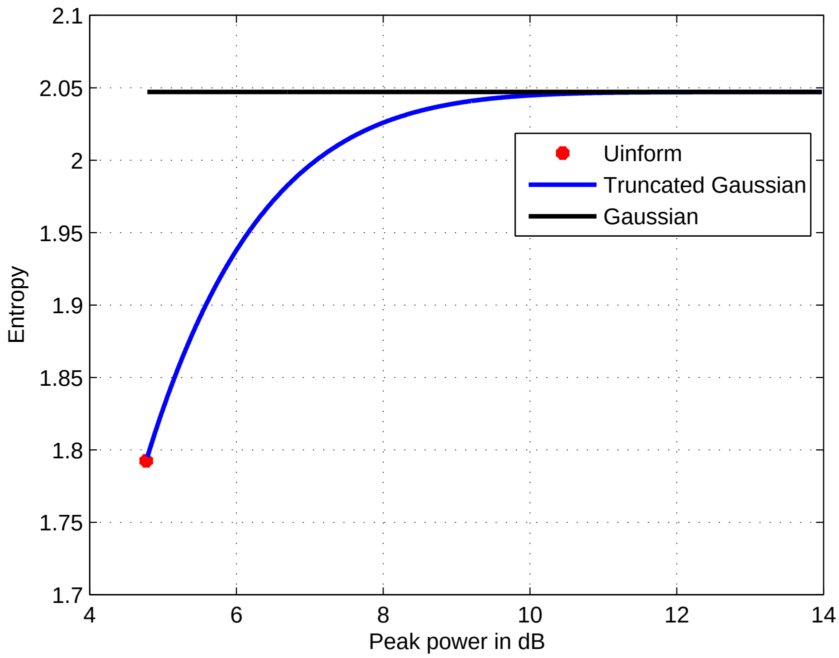

Figure 2.4: Differential entropy versus peak power, when the variance is one

2.2.3 The CCDF of PAPR for Output Sequence

Assume that the input sequence is filtered where the filter coefficients are deterministic and real, it is permitted to use the *sum of independent random variables theorem* [6] to compute the PDF and CCDF of PAPR for the output sequence analytically.

Sum of Independent Random Variable Theorem

According to the *sum of independent random variables theorem*, the PDF of the sum of two independent variables is the convolution of their PDFs. Assume that X and Y are two independent discrete random variables, the goal is to find the probability mass function of $Z = X + Y$. For example, given $Z = z$, X takes a certain value $X = k$ if and only if $Y = z - k$. The probability of $P(Z = z)$ is thus given by [6]

$$P\left(Z = z\right) = \sum_{k=-\infty}^{+\infty} P\left(X = k\right)\ P\left(Y = z - k\right) \tag{2.17}$$

In other words the PMF of Z is the convolution of the PMF of X and the PMF of Y. For continuous random variables X,Y and $Z = X + Y$, the PDF of Z is the convolution of the PDF of X and the PDF of Y. Note that X and Y

must be independent. Figure 2.5 depicts the PDF of the sum of two independent random variables with uniform distributions. The PDF of X is uniform on the interval $[-0.5, +0.5]$ and the PDF of Y is uniform on the interval $[-0.25, +0.25]$. The simulation results and analytical results are match.

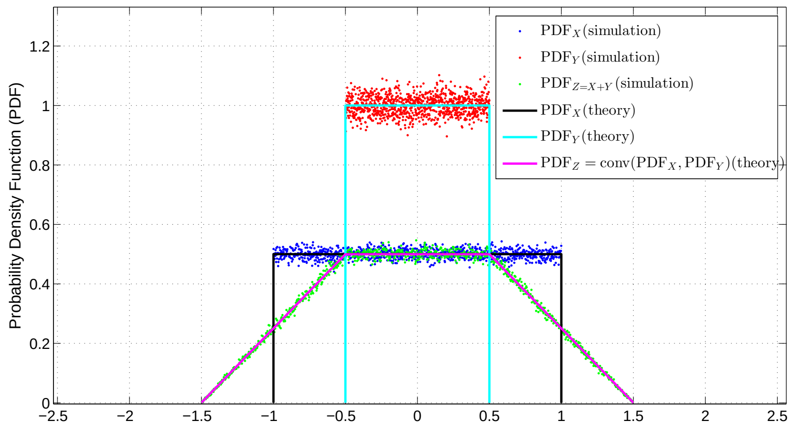

Figure 2.5: The PDF of the sum of two independent random variables which have uniform PDFs; dotted lines (.) are the simulation results and solid lines (-) are the analytical results

A sum of several independent random variables $S_n = X_1 + X_2 + ... + X_n$, can be rewritten as $S_n = S_{n-1} + X_n$, therefore according to Equation (2.17), the probability density function of S_n is given by the convolution of two PDFs

$$P_{S_n}(m) = \sum_{k=-\infty}^{+\infty} P_X(k)\, P_{S_{n-1}}(m-k) \tag{2.18}$$

where P_{S_n} is the PDF of S_n and P_X is the PDF of X. This equation formatting is very useful, because for an input sequence convolved with a filter which has $N+1$ deterministic coefficients, the probability density function of the output sequence is obtained by knowing the PDF of the input sequence. Assume that X is a random variable which can obtain any values of $x[k]$ on the interval $[-1, +1]$ with uniform PDF and $h = [\,h[0]\, h[1]\, \ldots\, h[N]\,]^T$, then the output sequence is

$$y[k] = h[k] * x[k] = \sum_{m=0}^{N} h[m]\, x[k-m] \tag{2.19}$$

Since the filter coefficients are deterministic, the output random variable Y is the sum of independent sequence of random variables

$$Y = h[0]X_0 + h[1]X_1 + ... + h[N]X_N = \sum_{k=0}^{N} h[k]X_k \tag{2.20}$$

where X_k is a random variable with the same PDF as random variable X.

The PDF of the scaled random variable $h[k]X_k$ can be calculated easily. Assume that $Y = aX$, where X is a random variable and a is a constant, then the PDF of Y is [6]

$$f_Y(y) = f_X(y/a)\ |\frac{\partial(y/a)}{\partial y}| \tag{2.21}$$
$$f_Y(y) = f_X(y/a)\ |\frac{1}{a}|$$

In Figure 2.5, $Y = 0.5X$, where X is a random variable with $uniform$ distribution sequence on the interval $[-1, +1]$ and as it is shown the $f_Y(y) = 2f_X(2y)$ is also a $uniform$ PDF but on the interval $[-0.5, +0.5]$. Therefore, the PDF of the output sequence can be calculated as the same way: the PDF of all scaled random variables ($h[k]X_k$, $k = 0, \ldots, N$) should be computed first and then they are convolved.

PDF of Squared Random Variable

The second step of computing the CCDF of PAPR is obtaining the PDF of squared of sum of independent random variables. If $Y = X^2$, then the probability of $P(Y \leq y)$ is

$$P(Y \leq y) = P(-\sqrt{y} \leq x \leq \sqrt{y}) \tag{2.22}$$

when X is a continuous random variable. The above equation can be rewritten as

$$P(Y \leq y) = P(x \leq \sqrt{y}) - P(x \leq -\sqrt{y}) \tag{2.23}$$

$$\mathrm{CDF}_Y(y) = \mathrm{CDF}_X(\sqrt{y}) - \mathrm{CDF}_X(-\sqrt{y}) \tag{2.24}$$

where CDF is *Cumulative Distribution Function*. Figure 2.6 shows a random variable X with uniform distribution on the interval $[-1, +1]$ and the PDF of $Y = X^2$.

PDF of PAPR for a Random Variable

The final step is to calculate the PDF of PAPR. In fact by having the PDF of the power of the output sequence, it is easy to compute the PDF or CCDF of PAPR, because the average power for a sequence is constant.

The CCDF of PAPR can be obtained from the PDF. As an example, consider an exemplary linear phase FIR filer $h = [-0.1250\ 0.2500\ -0.5000\ 1.0000\ -0.5000\ 0.2500\ -0.1250]^T$ (Figure 2.7) and input sequences for three types of PDF (uniform, Gaussian, truncated Gaussian) with same average power ($\sigma^2 = 1$) , the CCDF of PAPR of the input sequences are shown in Figure 2.8-(a) and the CCDF of PAPR for the output sequences are shown in Figure 2.8-(b).

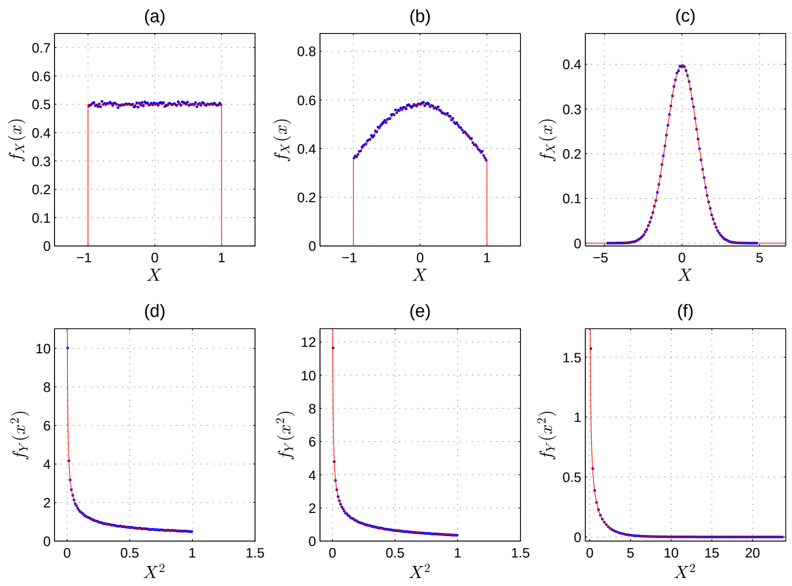

Figure 2.6: The PDF of X and $Y = X^2$; (a) uniform PDF, (b) truncated Gaussian PDF, (c) Gaussian PDF, (d), (e), (f) are the PDF of Y when X has uniform, truncated Gaussian and Gaussian distribution respectively. Dotted lines (.) are the simulation results and solid lines (-) are the analytical results

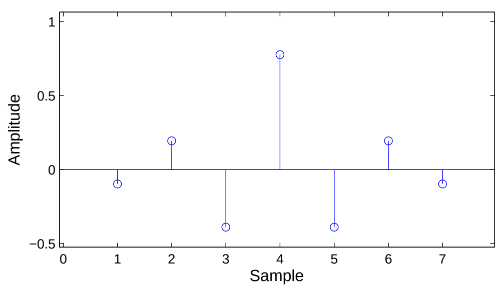

Figure 2.7: An exemplary linear phase FIR filter

For complex filters there is no straightforward way to compute the CCDF of PAPR analytically, since the real part and imaginary part of the filter output are not necessarily independent, the sum of independent random variables theorem is not satisfied.

2.3 PAPR Reduction Techniques

There are several techniques to reduce the PAPR of the transmit signal especially for OFDM systems. Some of these techniques are: clipping, tone reservation, tone

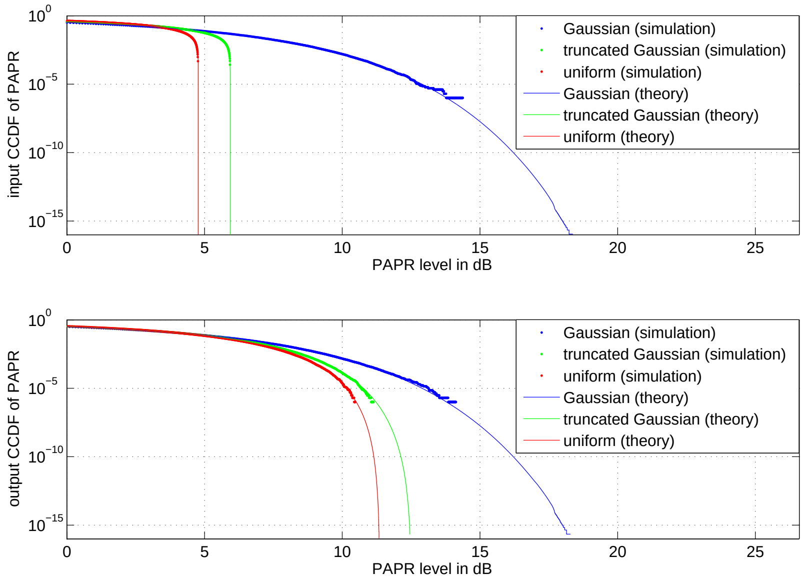

Figure 2.8: (a) The input CCDF of PAPR for the uniform, Gaussian and truncated Gaussian distribution sequences, (b) the output CCDF of PAPR; dotted lines (.) are the simulation results and solid lines (-) are the analytical results

injection, partial transmitted sequence, selected mapping, active constellation [2], [3], [5].

Note that the design of a filter with good PAPR-regrowth properties should not be seen as a PAPR reduction technique. The idea is to design a filter, which is already part of the chain to fulfil a certain purpose, in such a way to keep the PAPR-regrowth low. The following chapters of this thesis focus on such filter design methods based on the l_1-norm criterion.

3

l_1-Norm and Spectral Factorization Method

Linear filtering is usually a part of communication systems in order to shape signals properly and to remove noise and distortion. However as a consequence of the filtering process, the peaks of signals may regrow. Figure 2.8 shows that the PAPR of the filter output can increase considerably for an input data sequence with uniform or truncated Gaussian distribution.

In this Chapter, the focus is on the minimum l_1-norm approach to design filters with good PAPR properties. In the following sections the definition of the l_1-norm and the spectral factorization method are explained. It is assumed that the impulse response (or magnitude response) of the filter is given, since it is a part of the processing chain in communication systems. Therefore the autocorrelation function can be computed from the impulse response directly. In Section 3.2, the procedure of constructing all possible filters from a given autocorrelation function is explained.

3.1 l_1-Norm Definition

For a given filter $h = [\,h[0]\,h[1]\,\ldots\,h[N]\,]^T$, the l_1-norm is defined as following [4], [13]

$$||h||_1 = |h[0]| + |h[1]| + \cdots + |h[N]| = \sum_{n=0}^{N} |h[n]| \tag{3.1}$$

3.1.1 Support of the Output Sequence

The support of a sequence of data samples may change during the filtering process. Assume that $x = [\,x[0]\,x[1]\,\ldots\,x[M]\,]^T$ is an independent random input sequence limited on the condition $|x[n]| \leq B$, $n = 0, 1, \ldots, M$. The output sequence, which is a convolution of the input sequence and the filter coefficients, is given by

$$y[k] = \sum_{n=0}^{N} h[n]x[k-n] \tag{3.2}$$

then the absolute value of the output sequence is

$$|y[k]| = |\sum_n h[n]x[k-n]| \tag{3.3}$$

Since $|x[k-n]|$ is not greater than B, the output can be bounded by

$$|y[k]| \leq |\sum_n h[n]\, B| \tag{3.4}$$

Since B is a constant, then the above equation can be written as

$$|y[k]| \leq B\, |\sum_n h[n]\, | \tag{3.5}$$

The absolute value of the sum of the filter coefficients is not greater than the sum of the absolute values of the coefficients and thus

$$|y[k]| \leq B \sum_n |h[n]| = B\, ||h||_1 \tag{3.6}$$

As a result, for a bounded input sequence, the support of the output sequence is determined by the support of the input sequence and the l_1-norm of the filter [13]. Therefore a filter with lower l_1-norm may lead to a smaller output support

3.2 Autocorrelation Function and Spectral Factorization Method

For a given Finite Impulse Response (FIR) filter h of order N, the autocorrelation function $r = [\, r[-N] \, \ldots \, r[N]\,]^T$ is defined as

$$r[k] = \sum_n h[n]h[n+k] \tag{3.7}$$

The Power Spectral Density (PSD) of a sequence with autocorrelation function r is given by the Fourier transform of r

$$R(\omega) = \sum_k r[k]e^{-j\omega k} \tag{3.8}$$

For a Wide Sense Stationary (WSS) process, the power spectrum is real and positive, in the z-domain it can be factorized into a product form of its roots as following

$$R(z) = \sigma_0^2 H(z)H^*(\frac{1}{z^*}) \tag{3.9}$$

This factorization is called spectral factorization. σ_0^2 is the variance of the sequence. $H(z)$ is a rational minimum phase part of $R(z)$ and the roots of $H(z)$ are inside the unit circle. $H(\frac{1}{z})$ is the maximum phase part of the power spectrum which its all roots are located outside the unit circle [8]. The roots of the second part are conjugate reciprocal roots of the first part. Figure 3.1 depicts the roots of an exemplary autocorrelation function and the minimum phase part and the maximum phase part of its roots.

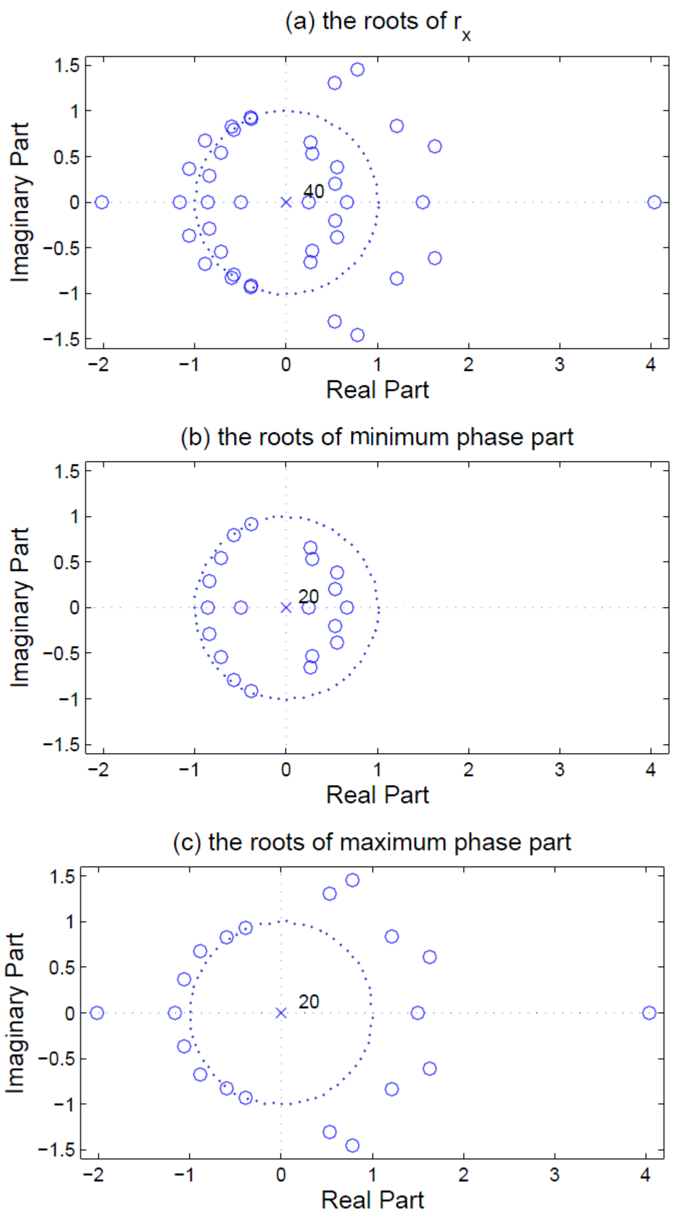

Figure 3.1: The roots of the autocorrelation function, the minimum phase part and the maximum phase part

Since the autocorrelation function is symmetric, it can be interpreted as the impulse response of a *linear-phase* FIR filter. Assume $P(z)$ is the Fourier transform of the autocorrelation function.

Complex-valued roots of real filters appear in complex-conjugate pairs (if α is root, so is α^*). Roots of symmetric filters appear in reciprocal pairs (if α is a root, so is α^{-*}). Thus, for a real symmetric filter $R(z)$ the following holds: If α is a real root of $R(z)$, then α^{-1} is also a root of $R(z)$. If α is a complex root of $R(z)$, then α^*, α^{-1}, and α^{-*} are also roots of $R(z)$.

According to Equation (3.9), for a filter of order N, its autocorrelation function has $2N$ roots where half of them are conjugate reciprocal roots of the rest. It is possible to construct a filter with the same autocorrelation function by taking a group of N-roots among $2N$ roots that does not contain any conjugate reciprocal roots. The number of all possible groups of N-roots that can construct filters with the same autocorrelation function is 2^N. In Figure 3.2-(a),(b), one group of N-roots is marked and its conjugate reciprocal roots are shown in part (c).

In the next part, the goal is to construct all possible filters with the same autocorrelation function corresponding to groups of N-roots and to find the filter with minimum l_1-norm.

3.3 Minimum l_1-Norm Filter

As mentioned in Section 3.1, a filter with minimum l_1-norm may cause lower peaks of the output sequence. Assuming that there is a given filter, which is already part of a communication system, the goal is to find the filter with minimum l_1-norm which has the same magnitude response as the given filter but may have different phase. In the following part the procedure of this method is explained [4]

- Compute the $2N$ roots of the polynomial of $r[k]\, z^{-k}$, $k = -N, \ldots, N$.
- Group all sets of N-roots among $2N$ roots that do not contain any conjugate reciprocal pairs.
- Construct the filters corresponding to all sets of N-roots.
- Scale the constructed filters h_k

$$h = \frac{\sqrt{r[0]}}{||h_k||_2}\; h_k \tag{3.10}$$

- Calculate the l_1-norm of the filters and find the filter with minimum l_1-norm.

The roots of the minimum l_1-norm filter for the given autocorrelation function in Figure 3.2-(a), are depicted in Figure 3.3. The frequency responses and the phases of the minimum phase filter and the minimum l_1-norm filter are shown in Figure 3.4. Two filters have the same magnitude responses, but their phases are different.

The output CCDF of PAPR of the minimum l_1-norm filter and the minimum phase filter are shown in Figure 3.5. The distribution of the input sequence is assumed to be uniform on the interval $[-0.5, +0.5]$. In this case, it can be seen that, the minimum l_1-norm filter has lower PAPR, and the asymptotic gain in PAPR is about 0.27dB.

However, the minimum l_1-norm filter does not always have a better performance in terms of PAPR, especially for high probabilities. For instance Figure 3.6

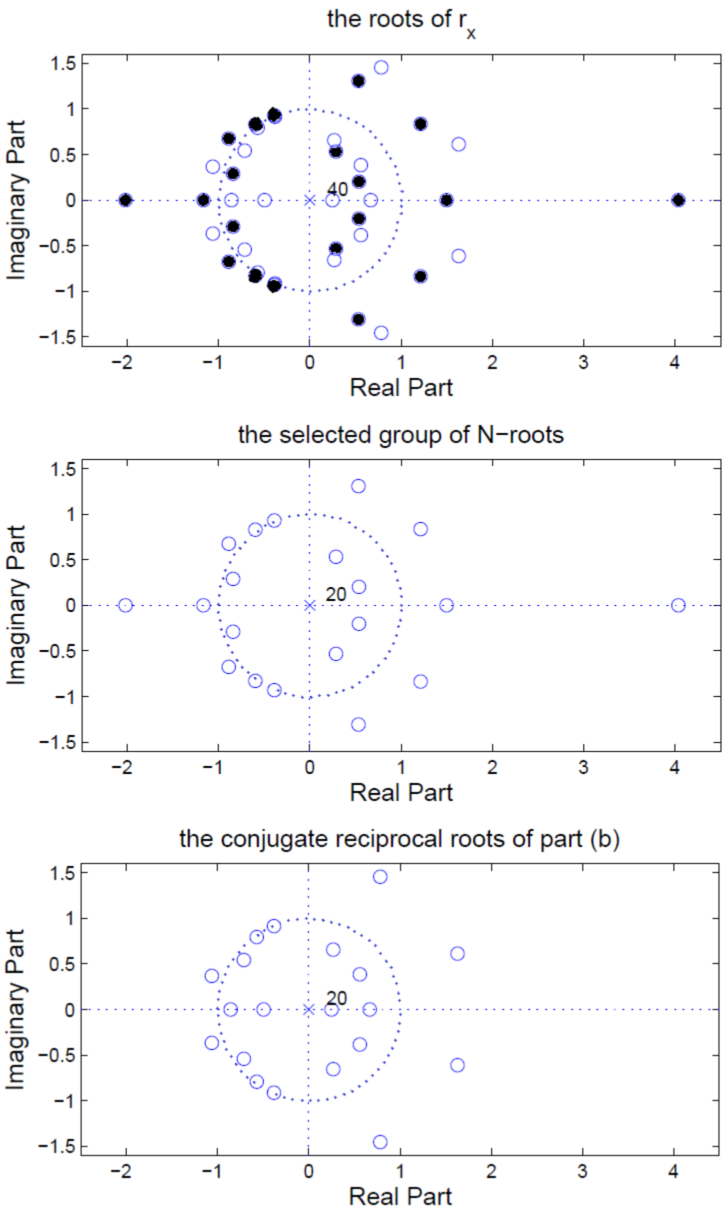

Figure 3.2: (a) The roots of the autocorrelation function, (b) a group of N-roots and (c) the conjugate reciprocal roots of part (b).

shows an example, the l_1-norm of the given least squares filter is 2.01 while the minimum l_1-norm is 1.92 numerically. But the minimum l_1-norm filter is worse than the least squares filter in PAPR gain for high probabilities. The frequency responses of the least squares filter and the minimum l_1-norm filter are depicted

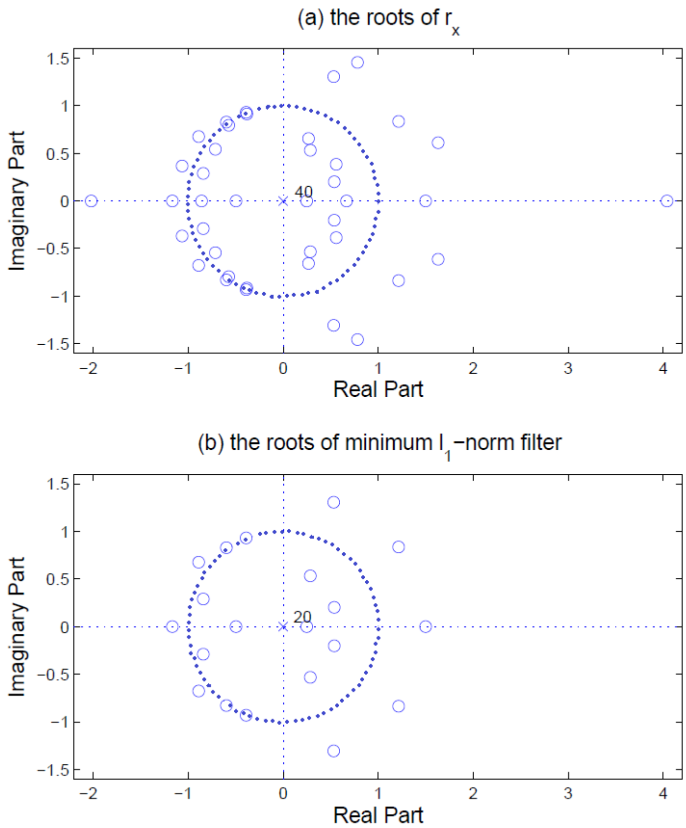

Figure 3.3: The roots of the autocorrelation function and the minimum l_1-norm filter

in Figure 3.8.

The second disadvantage of the spectral factorization method is computational complexity. For a given filter of order N, the number of filters that can be constructed from its autocorrelation function is 2^N. The spectral factorization method is not efficient for high order filters. The next chapter discusses the least squares filter design method and equiripple filter design method which are described as convex optimization based on l_1-norm criterion.

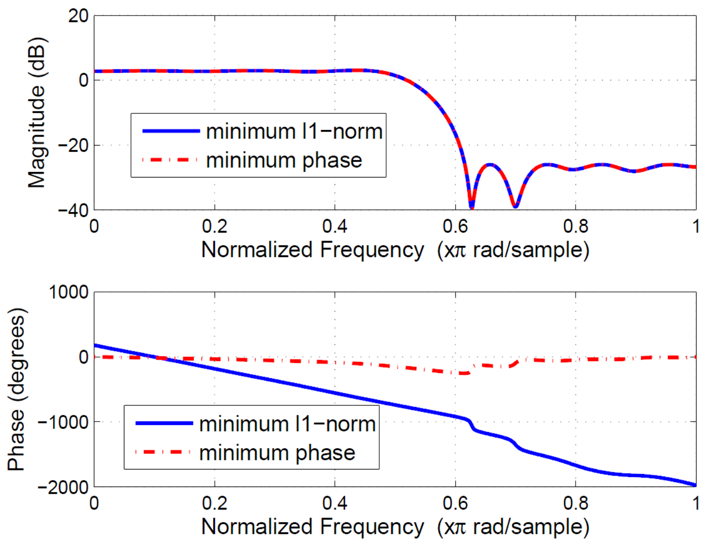

Figure 3.4: The frequency responses of the minimum l_1-norm filter and the minimum phase filter

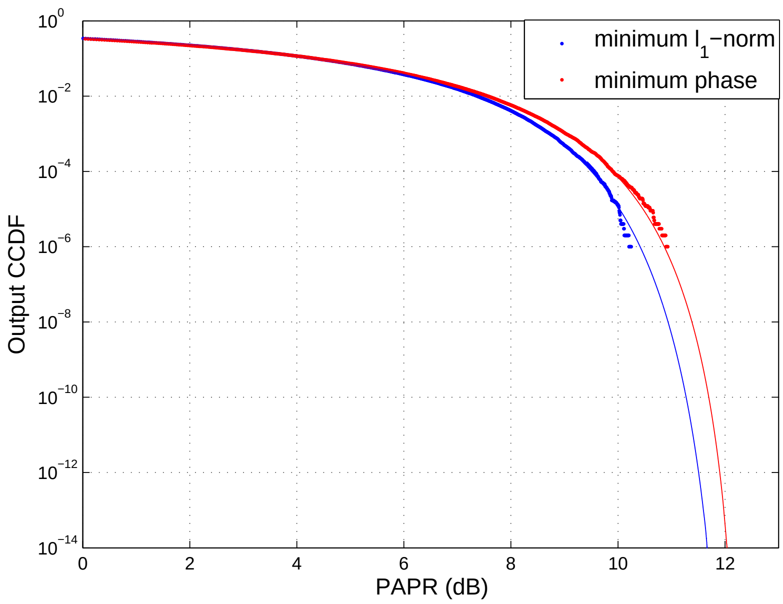

Figure 3.5: The output CCDF of PAPR of the minimum l_1-norm filter and the minimum phase filter

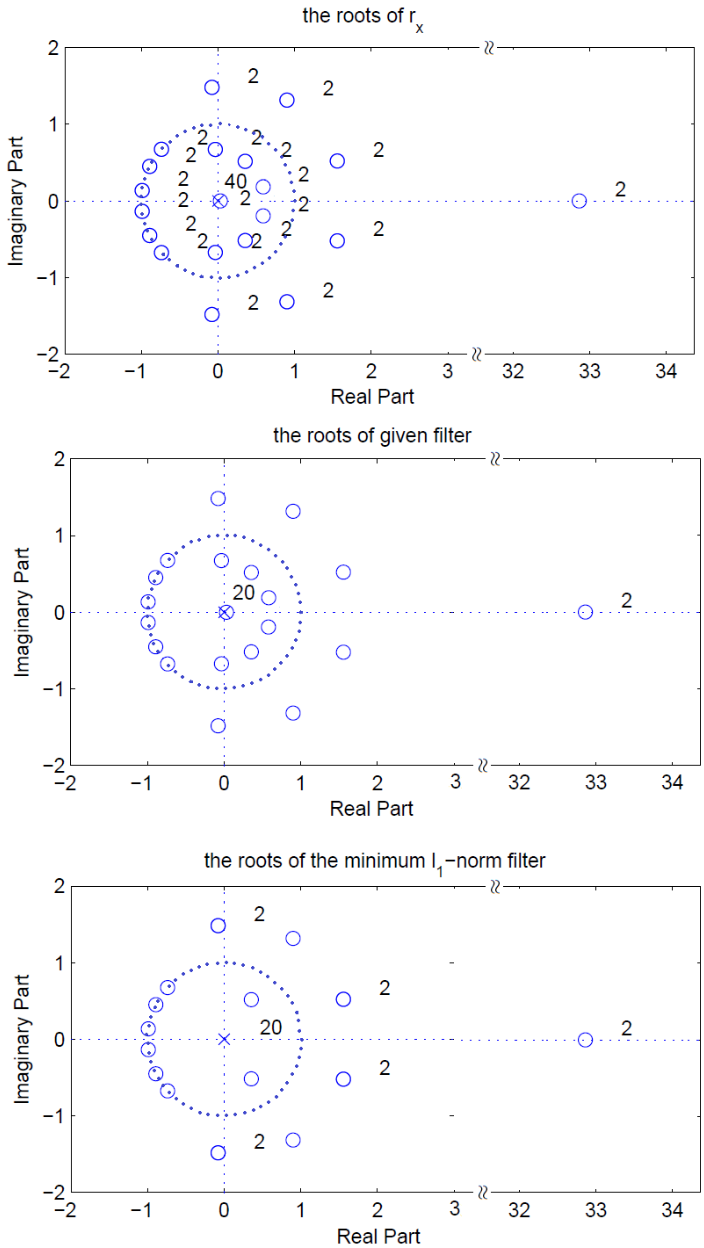

Figure 3.6: The roots of an exemplary given least squares filter and the minimum l_1-norm filter

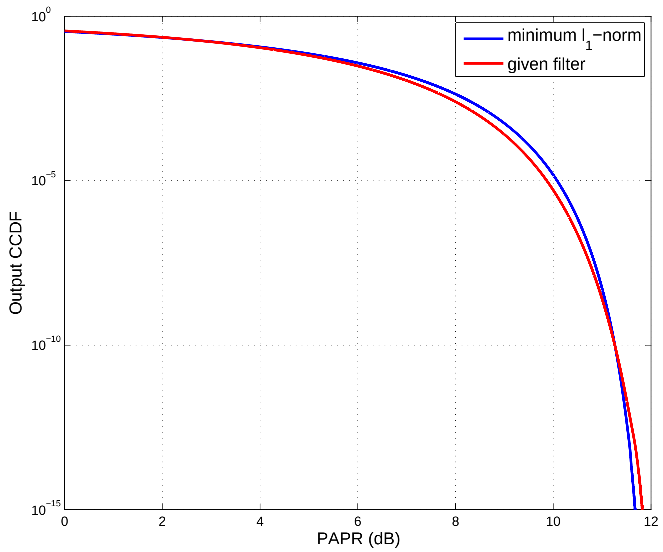

Figure 3.7: In some cases, the minimum l_1-norm filter does not have a better performance for high probabilities

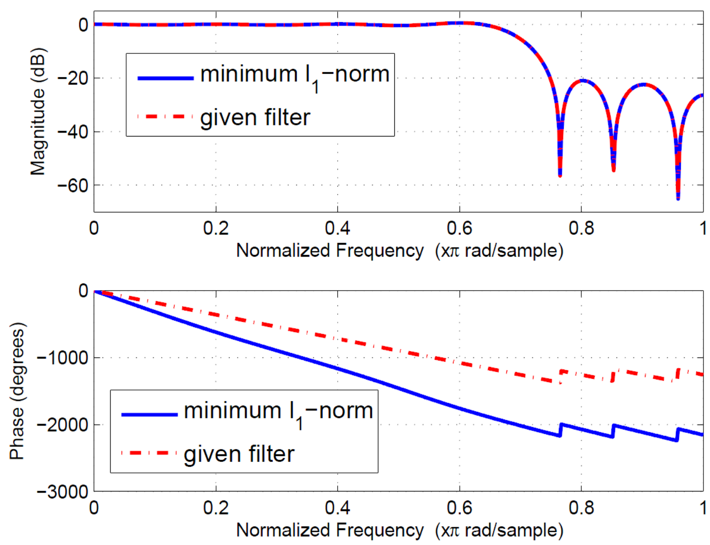

Figure 3.8: The frequency response of the given least squares filter and the minimum l_1-norm filter

4 Filter Design Using Convex Optimization

Convex optimization methods are well known and powerful tools to solve engineering problems in communication systems and they are applied in many areas such as filter design, optimal transmitter power allocation, phased-array antenna beam-forming and etc. These methods are efficient and reliable to solve a lot of problems directly or after converting them into convex forms. The goal of the convex optimization problem is to minimize an objective function subject to a set of convex constraint functions and affine functions [10], [11].

This chapter provides with a brief overview of convex optimization before focusing on filter design methods based on the l_1-norm criterion.

4.1 Convex Theory

4.1.1 Convex Sets

If any line between two points of a set C lies in C, it is a convex set, and it is defined as [10]

$$\theta x_1 + (1 - \theta)x_2 \in C, \tag{4.1}$$

where x_1 and x_2 can be any two arbitrary points of the set C, and $\theta \in [0, 1]$. In Figure 4.1 three sets are illustrated, the left one is convex and the other two sets are non-convex.

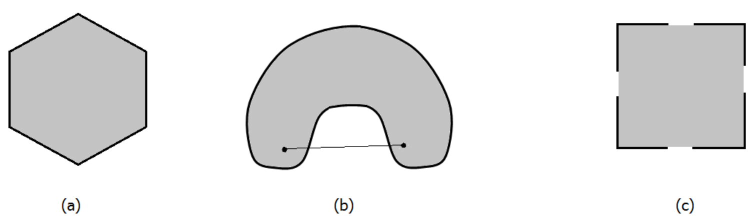

Figure 4.1: The set (a) is a convex set, the sets (b) and (c) are not convex [10]

4.1.2 Convex Function

A function $f : R^n \to R$ is a convex function if the following inequality is satisfied

$$f(\theta x + (1-\theta)y) \leq \theta f(x) + (1-\theta) f(y) \tag{4.2}$$

where $\theta \in [0, 1]$.

In words, Equation 4.2 states that for any point in the interval defined by the two points x and y, the function value is not greater than the line segment connecting x and y. A function is convex if Equation 4.2 holds for any two points in the domain of the function [10]. An example is given in Figure 4.2, any point of the line between two points $(x, f(x))$ and $(y, f(y))$ satisfies in Equation 4.2.

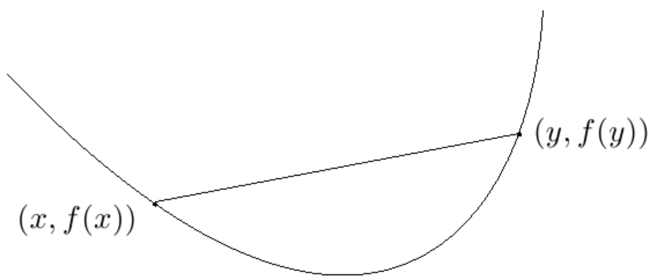

Figure 4.2: An example of convex function [10]

4.1.3 Convex Optimization Problem

A general form of an optimization problem is

$$\begin{array}{lll} \text{minimize} & f_0(x) & \\ \text{subject to} & f_i(x) \leq 0, & i = 1, \ldots, m \\ & h_i(x) = 0, & i = 1, \ldots, p \end{array} \tag{4.3}$$

where $x \in R^n$ is the *optimization variable* to minimize an *objective function* or *cost function*, $f_0(x) : R^n \to R$, subject to *inequality constraints* $f_i(x) \leq 0$, $i = 0, \ldots, m$ and *equality constraints* $h_i(x) = 0$, $i = 0, \ldots, p$. The special case when there are no constraints is called an *unconstrained* optimization problem. A Value x is called a feasible solution if $x \in C$ and satisfies the constraints $f_i(x)$ and $h_i(x)$. An optimization problem is a convex optimization problem if it is satisfied in three conditions [10]

- The objective function $f_0(x)$ is convex.

- The inequality functions $f_i(x) \leq 0$, $i = 0, \ldots, m$ are convex.
- The equality functions $h_i(x) = 0$, $i = 0, \ldots, p$ are affine functions.

An example of a convex optimization problem is minimizing the least squares error under the bounded constraints

$$\begin{array}{rl} \text{minimize} & \|\mathbf{A}x - b\|_2 \\ \text{subject to} & x \geq x_0 \\ & x \leq x_1 \end{array}$$

where x_0 is the lower bound of the feasible solution and x_1 is the upper bound.

4.2 Filter Design

In this section, *convex optimization* is used to design FIR filters with good PAPR properties. The optimization conditions are usually some constraints on the magnitude response of filters for pass-band and stop-band regions [12].

In the following section, two filter design methods are investigated. The first method is least squares filter design and the goal is to minimize the l_1-norm subject to a constraint on the sum of the squared error of the frequency response. The second method is equiripple filter design which minimizes the frequency error subject to an l_1-norm constraint. For simplicity the phases of the desired filters are linear for both methods.

4.2.1 Least Squares Design

Assume that $D(\omega)$ is the desired filter and $H(\omega)$ is the frequency response of the designed FIR filter $h = [\,h[0]\,h[1]\,\ldots\,h[N]\,]^T$ of order N

$$H(\omega) = \sum_{n=0}^{N} h[n]e^{-j\omega n} \tag{4.4}$$

The error in frequency domain, $E(\omega)$ is the difference of $D(\omega)$ and $H(\omega)$ which is defined as

$$E(\omega_i) = H(\omega_i) - D(\omega_i), \quad i = 0, \ldots, K \tag{4.5}$$

where $K + 1$ is the number of frequency points.

The frequency response in matrix notation is given by $H = \mathbf{A}\,h$, where $\mathbf{A}$ is the discrete Fourier transform matrix

$$\underbrace{\begin{bmatrix} H(\omega_0) \\ H(\omega_1) \\ . \\ . \\ . \\ H(\omega_K) \end{bmatrix}}_{H} = \underbrace{\begin{bmatrix} 1 & e^{-j\omega_0} & e^{-j2\omega_0} & \dots & e^{-jN\omega_0} \\ 1 & e^{-j\omega_1} & e^{-j2\omega_1} & \dots & e^{-jN\omega_1} \\ . & . & . & . & . \\ . & . & . & . & . \\ . & . & . & . & . \\ 1 & e^{-j\omega_K} & e^{-j2\omega_K} & \dots & e^{-jN\omega_K} \end{bmatrix}}_{\mathbf{A}} \underbrace{\begin{bmatrix} h[0] \\ h[1] \\ . \\ . \\ . \\ h[N] \end{bmatrix}}_{h} \tag{4.6}$$

The least squares solution minimizes the Euclidean norm of the error vector $[\,E(w_0)\,E(w_1)\,...\,E(w_K)\,]$ and is given by

$$\begin{aligned} h_{LS} = \arg\min_h \|E(\omega)\|_2 &= \arg\min_h \|D(\omega) - H(\omega)\|_2 \\ &= \arg\min_h \|D(\omega) - \mathbf{A}\,h\|_2 \end{aligned} \tag{4.7}$$

Assuming that $\mathbf{A}_{m\times n}$ is a skinny matrix $(\,m \geq n)$ and full rank, $\text{rank}(\mathbf{A}) = n$, the least squares solution given by the Moore-Penrose inverse [16] is

$$h_{\text{LS}} = \left(\mathbf{A}^H\mathbf{A}\right)^{-1}\mathbf{A}^H D \tag{4.8}$$

where $\mathbf{A}^H$ is the Hermitian conjugate matrix of $\mathbf{A}$.

l_1-Norm Minimization

The idea is to design a filter with good PAPR properties by minimizing the l_1-norm of the filter as an objective function subject to a constraint on the sum of the squared errors in frequency response. It is worth to note that both l_1-norm and sum of squared errors are convex function [10], therefore it is possible to define the problem as a convex form. The convex form of the least squares filter is

$$\begin{aligned} &\text{minimize} && \|h\|_1 \\ &\text{subject to} && \|D - \mathbf{A}h\|_2^2 \leq \epsilon \end{aligned}$$

The error ϵ is bounded from below by the conventional least squares error $\epsilon_{min} = \|D - \mathbf{A}h_{\text{LS}}\|_2^2$ where h_{LS} is the conventional least squares filter. If ϵ is equal to ϵ_{min}, the solution is h_{LS}, in which case there is no gain in l_1-norm compared to the conventional least squares filter.

In [13], the frequency error is determined by ϵ_{min} and a relaxation parameter, Δ, in order to achieve more freedom to minimize the l_1-norm.

$$\begin{aligned} &\text{minimize} && \|h\|_1 \\ &\text{subject to} && \|D - \mathbf{A}h\|_2^2 \leq \epsilon_{min} + \Delta \end{aligned}$$

Larger values of the relaxation parameter lead to smaller l_1-norms at the cost of larger errors in frequency response. The proposed D in [13] is a complex desired filter which has a magnitude and a phase in frequency domain, however finding the proper phase for the filter is still a problem. In many applications the phase of the filter is not important, and it is more convenient to assume a zero-phase for the desired magnitude response [14]. But a zero-phase for the desired magnitude response is not an optimal solution.

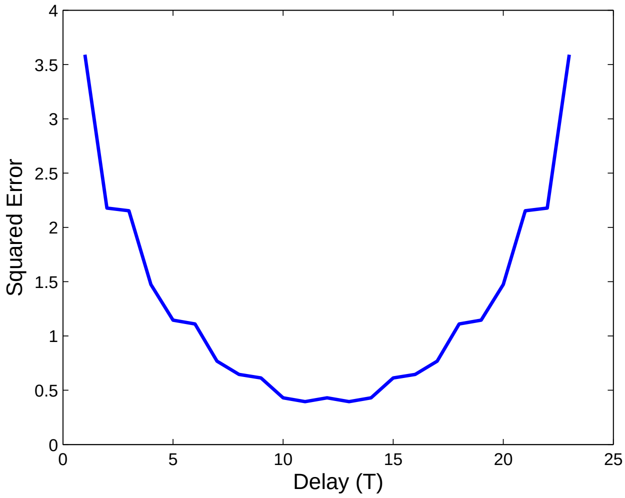

Figure 4.3: Sum of squared error of the designed filters versus different time delays (T) for the given magnitude response

In [9] for the different types of linear-phase filters, the phase is defined as $e^{-j\omega\frac{N}{2}}$, where N is the order of the filter. However, for a given magnitude response, the linear phase can be defined as $e^{-j\omega T}$, where T is a time delay. Different time delays can provide a possibility to achieve different linear-phases for the given magnitude response. Figure 4.3 depicts sum of squared error of the designed filters versus different time delays (T) for the exemplary given magnitude response. Usually the optimal value of time delay is $T = \frac{N}{2}$. In this thesis, the phase of the given magnitude response is linear and it is defined as $e^{-j\omega\frac{N}{2}}$.

An example is given in order to have a good evaluation of the least squares filter design method with a relaxation parameter. The order of the filter is $N = 24$, the pass-band frequency and the stop-band frequency are defined as $[0,\, 0.3\pi]$ and $[0.4\pi,\, \pi]$, respectively. Figure 4.4 shows the output CCDF of PAPR of the filters with different relaxation parameters.

The asymptotic gain in PAPR for $\Delta = 3\epsilon_{min}$ and $\Delta = 8\epsilon_{min}$ compared to the conventional least squares filter ($\Delta = 0$) are about 0.35dB and 0.8dB, respectively. The details of the frequency responses of the designed filters are depicted in Figure 4.5. According to Table 4.1 for the larger values of Δ, the errors of magnitude response will increase in all frequency bands.

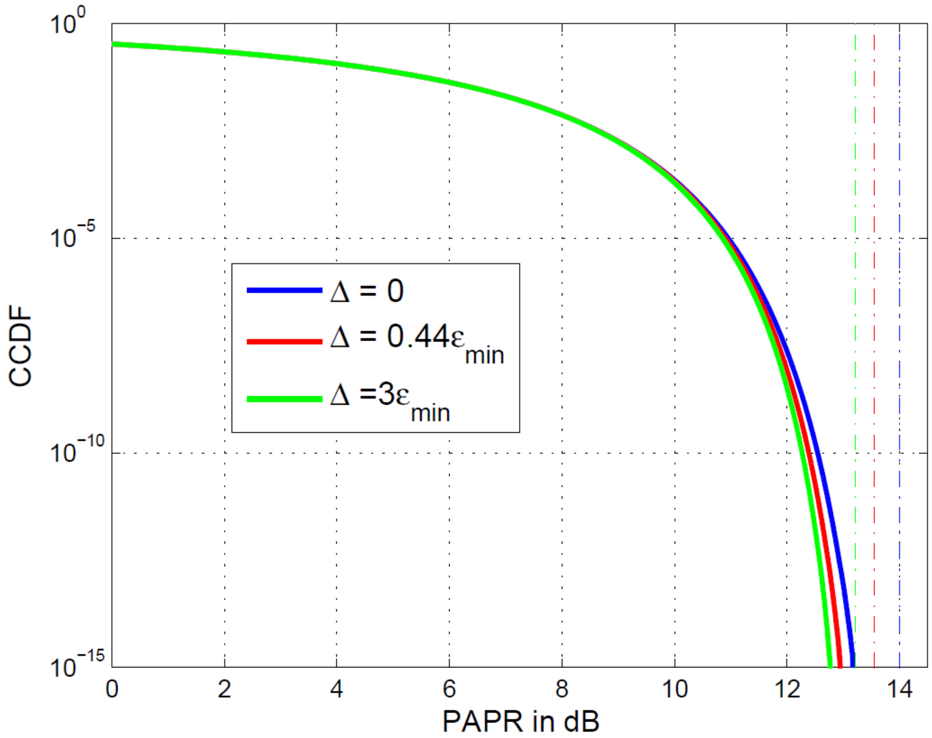

Figure 4.4: The output CCDF of PAPR of the filters with different relaxation parameters

4.2.2 Equiripple FIR Filters

Equiripple FIR filters are popular since they have an acceptable frequency response in the transition band and moderate deviations for pass-band and stop-band frequencies. This method tries to minimize the maximum errors in each frequency band. The *Remez exchange algorithm* is one of the efficient iterative methods to achieve an optimal filter in the above sense [9] [15].

Assume the filter h of order N is linear-phase and type-I (N is even), then the impulse response of the filter is symmetric; $h[n] = h[N-n]$, $n = 0, \ldots, \frac{N}{2}$. For type-I filters, $H(\omega)$ can be written according to [9] as

$$H(\omega) = e^{-j\omega\frac{N}{2}} A(\omega) \tag{4.9}$$

where the amplitude function $A(\omega)$ is given by

$$A(\omega) = \sum_{k=0}^{\frac{N}{2}} g[k] \cos(k\omega) \tag{4.10}$$

Table 4.1: The comparison of least squares filters with different relaxation parameters

Sum of squared error	$\epsilon_{min} = 2.0450$ ($\Delta = 0$)	$1.44\epsilon_{min} = 2.9448$ ($\Delta = 0.44\epsilon_{min}$)	$4\epsilon_{min} = 8.1800$ ($\Delta = 3\epsilon_{min}$)
Asymptotic gain in PAPR	0dB	0.35dB	0.8dB
Maximum pass-band error	0.87dB	1.54dB	1.84dB
Maximum stop-band error	4.6dB	4.6dB	6.3dB
Stop-band frequency deviation ($\times\pi$ rad/sample)	0.0183	0.0216	0.0281
Attenuation at stop-band edge	−25.9dB	−25.45dB	−21.77dB

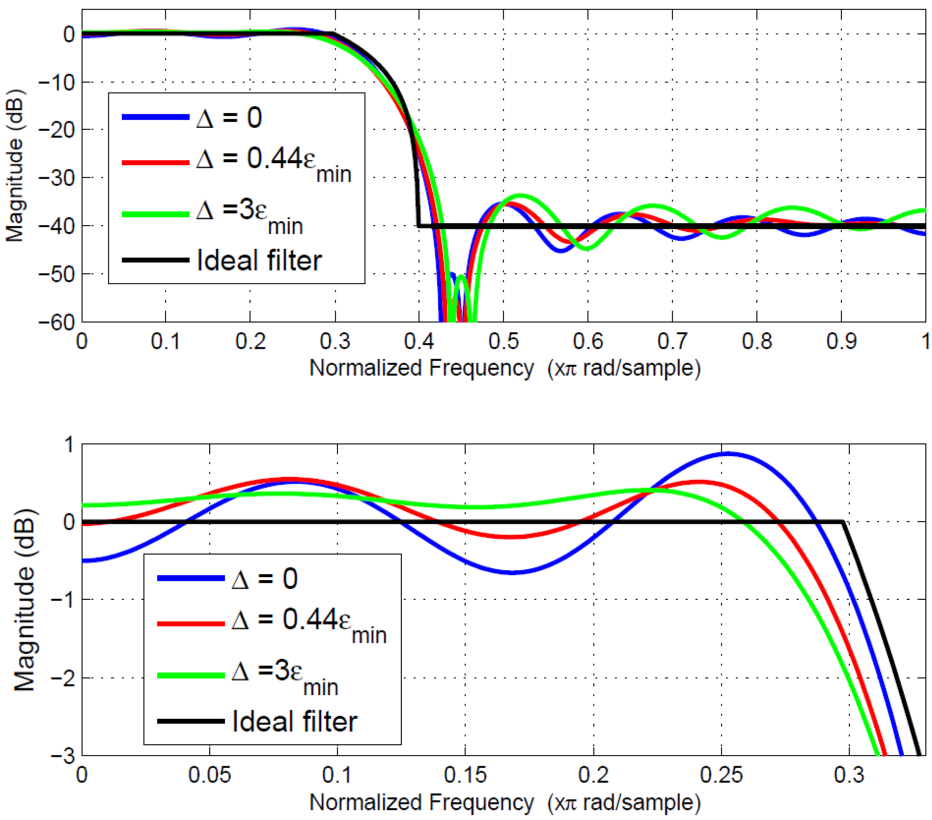

Figure 4.5: The frequency responses of the designed least squares filters with different relaxation parameters

where g can be obtain from h

$$g[0] = h[\frac{N}{2}]$$
$$g[k] = 2h[\frac{N}{2} - k], \quad k = 1, \ldots, \frac{N}{2} \tag{4.11}$$

The weighted frequency response error is

$$E(\omega) = V(\omega)(A(\omega) - D(\omega)) \tag{4.12}$$

$V(\omega)$ is non-negative weight and $D(\omega)$ is the amplitude of the desired filter. The optimization problem to minimize the frequency errors in pass-band and stop-band regions is known as *minmax* problem [9]

$$\epsilon = \underset{g}{\text{minimize}} \max |E(\omega)| \tag{4.13}$$

According to *the alternation theorem* there is a unique optimal solution, where $E(\omega)$ is equiripple at $\frac{N}{2} + 1$ frequency points [9]

$$\begin{aligned} |E(\omega_i)| &= \epsilon, && \text{for } i = 0, \ldots, \frac{N}{2} + 1 \\ E(\omega_{i+1}) &= -E(\omega_i), && \text{for } i = 0, \ldots, \frac{N}{2} \end{aligned} \tag{4.14}$$

Then the Equation (4.12) can be written as

$$V(\omega_i)(A(\omega_i) - D(\omega_i)) = (-1)^i \epsilon, \quad \text{for } i = 0, \ldots, \frac{N}{2} + 1 \tag{4.15}$$

It is useful to define the matrix form of the above equation as $\mathbf{A}_{\text{eq}}\, g_{\text{eq}} = D$ where

$$\underbrace{\begin{bmatrix} 1 & \cos(\omega_0) & \cos(2\omega_0) & \ldots & \cos(\frac{N}{2}\omega_0) & \frac{1}{V(\omega_0)} \\ 1 & \cos(\omega_1) & \cos(2\omega_1) & \ldots & \cos(\frac{N}{2}\omega_1) & \frac{-1}{V(\omega_1)} \\ . & . & . & . & . & . \\ . & . & . & . & . & . \\ . & . & . & . & . & . \\ 1 & \cos(\omega_{\frac{N}{2}+1}) & \cos(2\omega_{\frac{N}{2}+1}) & \ldots & \cos(\frac{N}{2}\omega_{\frac{N}{2}+1}) & \frac{(-1)^{\frac{N}{2}+1}}{V(\omega_{\frac{N}{2}+1})} \end{bmatrix}}_{\mathbf{A}_{\text{eq}}} \underbrace{\begin{bmatrix} g[0] \\ g[1] \\ . \\ . \\ . \\ g[\frac{N}{2}] \\ \epsilon \end{bmatrix}}_{g_{\text{eq}}} = \underbrace{\begin{bmatrix} D(\omega_0) \\ D(\omega_1) \\ . \\ . \\ . \\ D(\omega_{\frac{N}{2}}) \\ D(\omega_{\frac{N}{2}+1}) \end{bmatrix}}_{D} \tag{4.16}$$

The Remez algorithm is an iterative interpolation method to achieve the optimal solution of the problem which has lower computational complexity than finding the matrix-form solution [9]. However, it is not possible to directly deploy the Remez algorithm to design a filter subject to an l_1-norm constraint. The convex form of the equiripple filter can be one approach to reach this goal. In the following section the l_1-norm is used as a constraint in convex problem formulation to design equiripple filters.

l_1-Norm Constraint

The idea of the convex form in the equiripple filter design is to minimize the frequency response error in Equation 4.16 subject to a constraint on the l_1-norm of the filter as following

$$\begin{aligned} &\text{minimize } \|\mathbf{A}_{\text{eq}}(\omega_i)g_{\text{eq}} - D(\omega)\|_2, \\ &\text{subject to } \|h\|_1 \leq \textit{threshold} \end{aligned} \tag{4.17}$$

where h is the filter defined in Equation (4.11). The upper bound *threshold* can be determined by the l_1-norm of the filter which does not have any constraint on $\|h\|_1$.

Figure 4.6 illustrates the output CCDF of PAPR of the three equiripple filters with different constraints on their l_1-norm. The order of each filter is $N = 77$, the pass-band frequency and the stop-band frequency are defined as $[0, 0.48\pi]$ and $[0.59\pi, \pi]$, respectively. There is no *threshold* for the unconstrained filter h_1 and its l_1-norm is equal to $\|h_1\|_1 = 1.9401$ numerically. The *threshold* for the filter with a constraint should be smaller than $\|h_1\|_1$. For the two example filters, the l_1-norm constraint is set to $0.95\|h_1\|_1$ and $0.9\|h_1\|_1$, respectively. As shown in Figure 4.6 the CCDF of PAPR decreases for the filter with smaller l_1-norm. The asymptotic gains in PAPR for the filters with $0.95\|h_1\|_1$ and $0.9\|h_1\|_1$ constraints on their l_1-norm are about 0.37dB and 0.76dB, respectively. The frequency responses of these filters are depicted in Figure 4.7 and clearly show that the cost of achieving a gain in PAPR is a larger error in the frequency response. The main errors appear near the transition band. The smaller the *threshold* in the l_1-norm constraint, the larger is the error in frequency. Table 4.2 illustrates the gain in PAPR and frequency response errors in different bands for different constraints on l_1-norm.

In the next chapter, the three filter design methods will be compared in terms of PAPR gain and frequency error.

Table 4.2: The comparison of equiripple filters with different l_1-norm constraints

Threshold	$\|h_1\|_1 = 1.9401$	$0.95\|h_1\|_1 = 1.8431$	$0.9\|h_1\|_1 = 1.7461$
Asymptotic gain in PAPR	0dB	0.37dB	0.76dB
Maximum pass-band error	0.1dB	0.94dB	1.59dB
Maximum stop-band error	4.2dB	4.7dB	6.5dB
Stop-band frequency deviation ($\times\pi$ rad/sample)	0.001	0.010	0.025
Attenuation at stop-band edge	−36.8dB	−26.25dB	−21.8dB

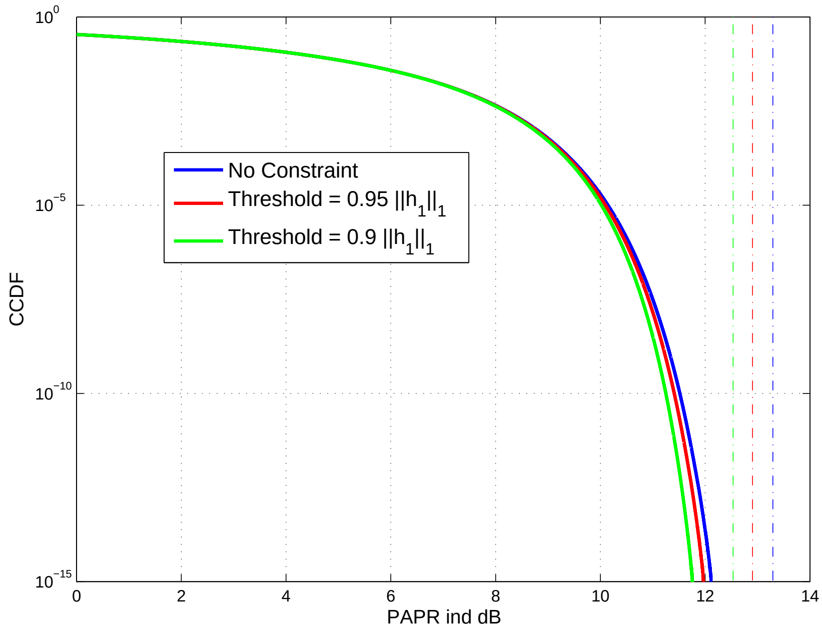

Figure 4.6: The output CCDF of PAPR of the equiripple filters with different thresholds

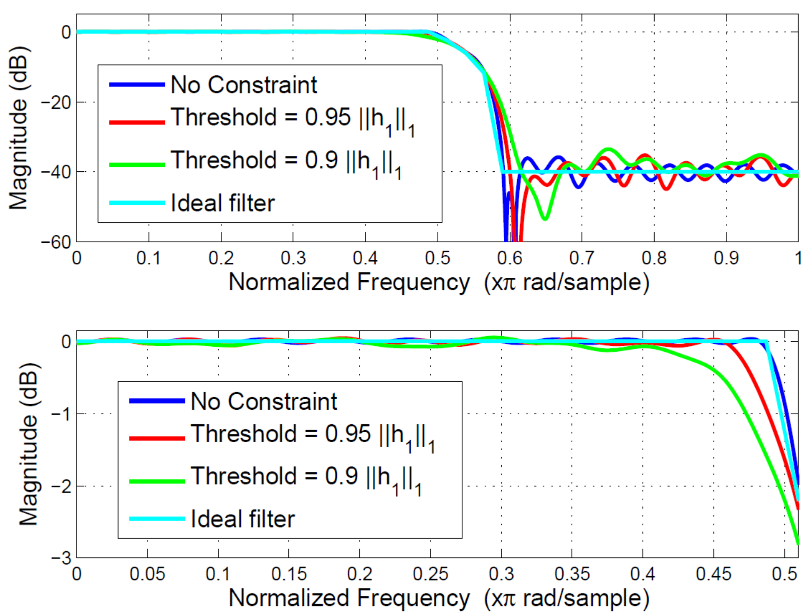

Figure 4.7: The frequency responses of the equiripple filters with different thresholds

5 Comparisons

In this chapter, three filter design methods are compared in terms of PAPR gain and frequency response error:

- spectral factorization method
- least squares filter design cast as convex problem
- equiripple filter design cast as convex problem.

The theories and details of these methods are explained in the previous chapters.

In order to ensure a fair comparison of the three methods, it is assumed the order of each filter is not greater than $N = 24$. This choice is motivated by the computational complexity of the spectral factorization method, which increases exponentially with the order of the filter. In the following, three examples are evaluated. In each example, the designed filter using the spectral factorization method has a different PAPR gain compared to the conventional least squares filter. The magnitude response of the desired filter is given in these examples.

In the first example, the output CCDF of PAPR of the spectral factorization method has a gain in PAPR about 0.3dB. The order of the filters are $N = 24$, the pass-band frequency and the stop-band frequency are defined as $[0, 0.54\pi]$ and $[0.62\pi, \pi]$, respectively. In order to achieve same gains in PAPR in all three methods, it is necessary to choose proper values for Δ in the least squares method with a relaxation parameter and also for *threshold* in the equiripple method. Figure 5.1 shows the output CCDF of PAPR of all filters. The three designed filters have same gains in PAPR compared to the conventional least squares filter.

In Figure 5.2 the frequency responses of the designed filters are illustrated. All filters have some errors compared to the desired filter. However the errors of the conventional least squares filter and the minimum l_1-norm filter are smaller than the errors of the other two filters especially near the transition band. The frequency errors of the minimum l_1-norm filter and the conventional least squares filter are the same, since they have same magnitude responses but different phases. According to the results of Table (5.1) the performance of the minimum l_1-norm filter is better than the least squares filter with a relaxation and the equiripple filter in all frequency bands. On the other hand, the equiripple filter has better

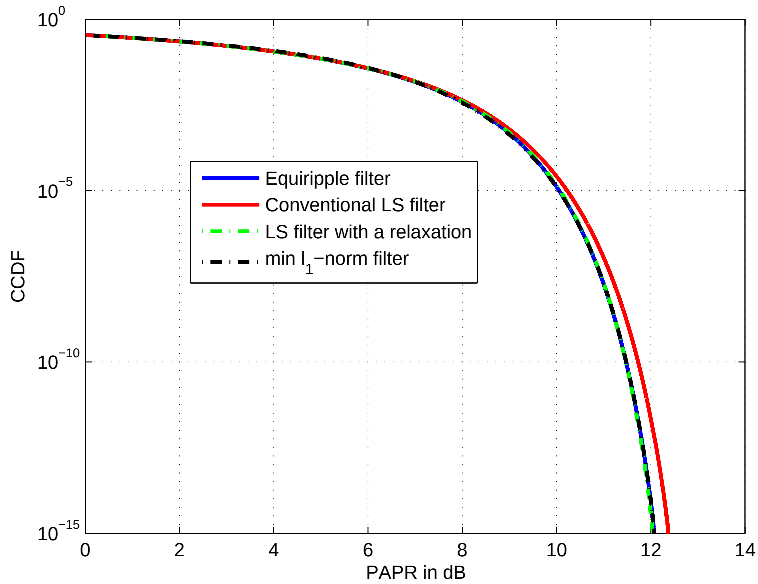

Figure 5.1: The output CCDF of PAPR of the three different filters [example 1]

performance than the least squares filter with a relaxation in pass-band and transition band, but it is worse in stop-band. Therefore, in this example, the minimum l_1-norm filter is superior to the other filters.

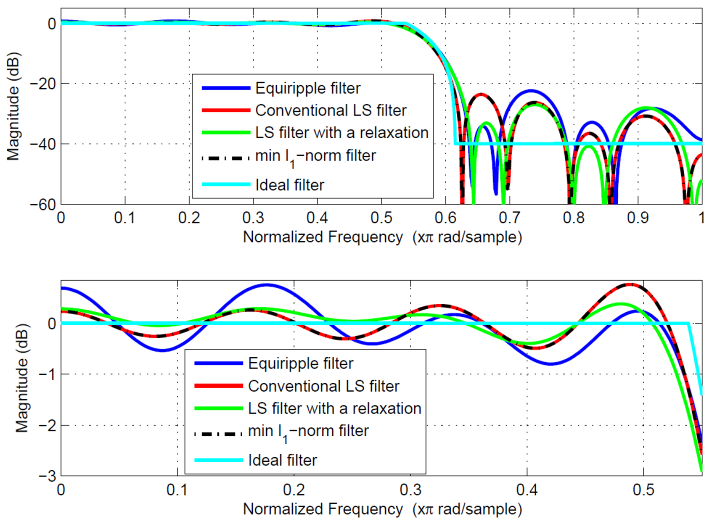

Figure 5.2: The frequency response of the three different filters [example 1]

Table 5.1: The comparison of filter design methods in terms of PAPR gains and frequency response errors

Filter design methods	Conventional LS	Minimum l_1-norm	LS with relaxation	Equiripple design
Asymptotic gain in PAPR	0dB	0.3dB	0.3dB	0.3dB
Maximum pass-band error	1.09dB	1.09dB	1.52dB	1.36dB
Maximum stop-band error	13.3dB	13.3dB	13.4dB	16.3dB
Stop-band frequency deviation ($\times\pi$ rad/sample)	0.0222	0.0222	0.0360	0.0318
Attenuation at stop-band edge	-17.1dB	-17.1dB	-14.92dB	-15.47dB

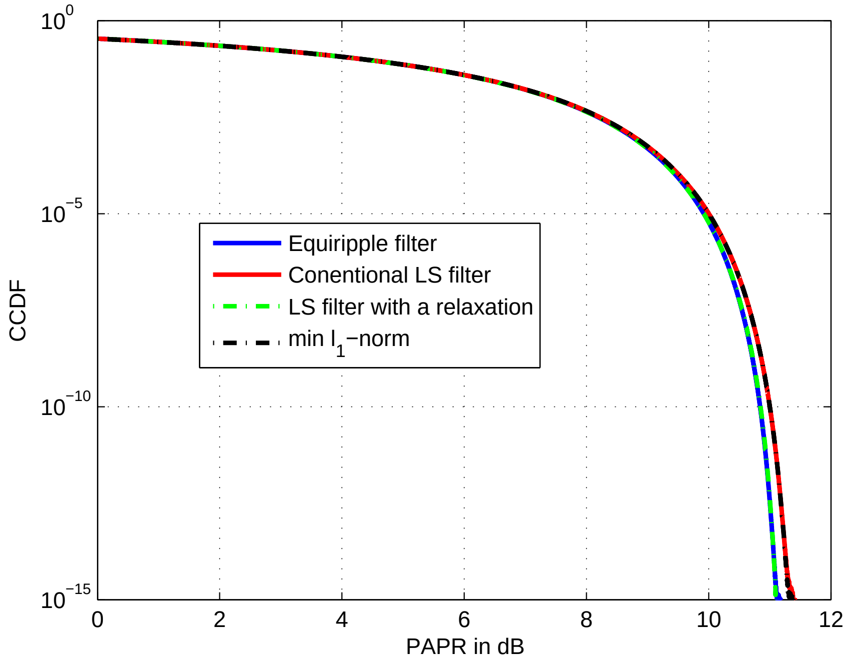

Figure 5.3: The output CCDF of PAPR of the three different filters [example 2]

In the second example, the order of each filter is $N = 22$, and the frequency bands for pass-band and stop-band are $[0, 0.42\pi]$ and $[0.58\pi, \pi]$, respectively. In this example the minimum l_1-norm filter using spectral factorization method does not have any PAPR gain compared to the conventional least squares filter, but for the other two filters which are cast convex problem the asymptotic PAPR gains are about 0.24dB (Figure 5.3). The relaxation parameter (Δ) and *threshold* are chosen in such a way that these methods have same gains in PAPR.

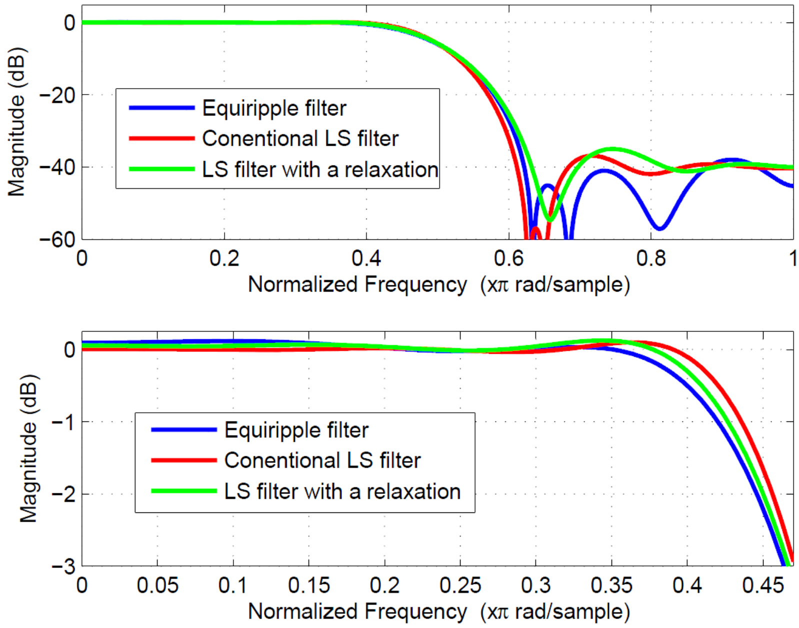

Figure 5.4: The frequency response of the three different filters [example 2]

In this scenario, the equiripple filter has better performance than the least squares filter with a relaxation in transition band and stop-band, but it is worse in pass-band.

And finally, in the third example, the order of the filters are $N = 22$, and the frequency bands for pass-band and stop-band are defined as $[0, 0.17\pi]$ and $[0.42\pi, \pi]$, respectively. In this scenario the minimum l_1-norm filter has worse performance in terms of PAPR gain compared to the conventional least squares filter for high probabilities. Figure 5.5 depicts the CCDF of PAPR of the different design methods. The filters described as convex problem have same gains in PAPR (about 0.2dB).

The magnitude responses of the equiripple filter and the least squares filter with a relaxation do not differ much in different frequency bands (Figure 5.6). However the cost for achieving gain in PAPR is extra frequency error in transition band.

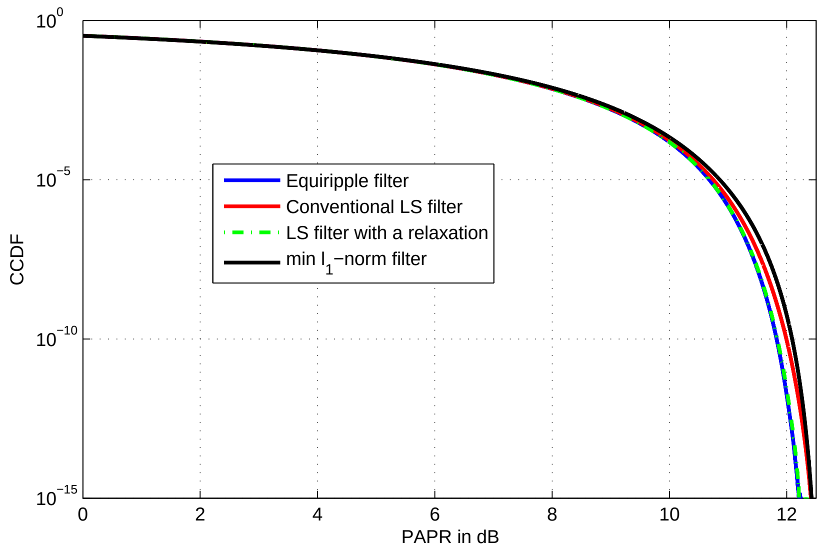

Figure 5.5: The output CCDF of PAPR of the three different filters [example 3]

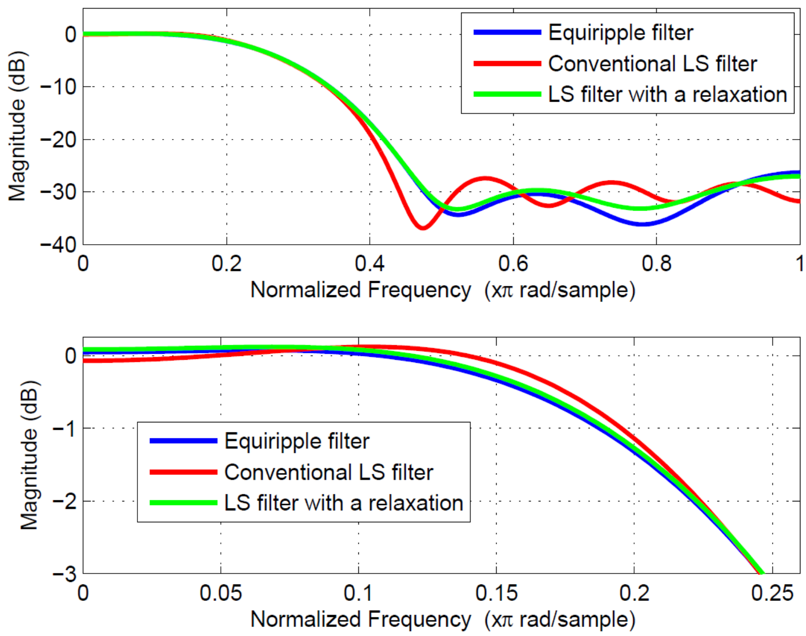

Figure 5.6: The frequency response of the three different filters [example 3]

According to the three evaluation results, the minimum l_1-norm filter using the spectral factorization method can be chosen as the best method when it has a gain in PAPR. Although this method does not have a good performance for high order filters. In other cases, the equiripple filter is cast convex problem has better performance than the least squares filter with a relaxation in transition band but it is usually worse in other frequency bands. However for those filters are described as convex problem there is a trade-off between achieving gain in PAPR and frequency response error.

6 Conclusions and Further Work

6.1 Summary and Conclusions

The minimum l_1-norm criterion has been considered as an approach to design filters that keep the PAPR regrowth low. Three different filter design methods are investigated in this thesis. Each of them has some advantages and disadvantages.

The spectral factorization method usually works well for filters with orders of up to $N = 24$. It should be mentioned that in some cases this method does not yield any gain in PAPR.

Convex optimization is a powerful tool to design filters given certain constraints. Two different filter design approaches employing convex optimization are investigated. First, the least squares method with a relaxation parameter in frequency error and l_1 minimization is considered. Second, the equiripple method, which minimizes the error in frequency-domain subject to an l_1-norm constraint is investigated. It is possible to improve PAPR properties of the filtered signal with both methods, but at the cost of an error in frequency response. The equiripple design method has a lower error than the least squares method with a relaxation error in transition band and pass-band, but it is worse in stop-band frequencies.

The obtained gain in PAPR is usually less than 1dB, especially for spectral factorization method, although for the two other methods it is possible to reach a gain in PAPR of more than 1dB by accepting a larger error in frequency response.

6.2 Further Work

In this thesis, it has been assumed that the phase of filters is linear. Non-linear phase filters can provide more freedom to minimize the l_1-norm. Finding the best phase in the sense of minimizing the PAPR of the filtered signal is a complicated problem.

The focus of this thesis has been on real filters, but the l_1-norm criterion can be evaluated for complex filters.

References

[1] T. Hwang, C. Yang, G. Wu, S. Li, and G. Ye Li, *OFDM and its Wireless Applications: A Survey*, IEEE Transactions on Vehicular Technology, Vol. 58, No. 4, May 2009.

[2] N. Andgart, *Peak and Power Reduction in Multi-carrier Communication Systems*, PhD. Thesis, Department of Information Technology, Lund University, Sweden, Nov. 2005.

[3] T. Jiang, Y. Wu, *An Overview:Peak-to-Average Power Ratio Reduction Techniques for OFDM Signals*, IEEE Transactions on Broadcasting, Vol. 54, No. 2, June 2008.

[4] T. Magesacher, J. M. Cioffi, *On Minimum Peak-to-Average Power Ratio Spectral Factorization*, Multi-Carrier Systems and Solutions (MC-SS), 2011 8th International Workshop on.

[5] V. Vijayarangan, R. Sukanesh, *An Overview of Techniques for Reducing Peak to Average Power Ratio and its Selection Criteria for Orthogonal Frequency Division Multiplexing Radio System*, Journal of Theoretical and Applied Information Technology, Vol. 5, No. 1, 2009

[6] C. M. Grinstead, J. L. Snell, *Introduction to Probability*, Second Edition, 1997.

[7] T. Magesacher, *OFDM for Broadband Communication*, Department of Electrical and Information Technology, Lund University, 2011.

[8] A. H. Sayed, and T. Kailath, *A Survey of Spectral Factorization Methods*, Numerical Linear Algebra With Applications, Linear Algebra April, 2001.

[9] B. Porat, *A Course in Digital Signal Processing*, Joh Wiley & Son Inc, 1997.

[10] S.-P. Wu, S. Boyd, and L. Vandenberghe, *Convex Optimization*, Cambridge University Press, Seventh Edition, 2009.

[11] Z. Luo,W. Yu, *An Introduction to Convex Optimization for Communications and Signal Processing*, IEEE Journal on Selected Areas in Communications, Vol. 24, No. 8, August 2006.

[12] S.-P. Wu, S. Boyd, and L. Vandenberghe, *FIR Filter Design via Spectral Factorization and Convex Optimization*, Chapter 5 in Applied and Computational Control, Signals and Circuits, pp. 215–245, 1998.

[13] C. Tseng and S. Lee, *Design of FIR Filter Using Constrained l_1 Minimization Method*, TENCON 2009 - 2009 IEEE Region 10 Conference.

[14] A. E. Cetin, Ö. N. Gerek and Y. Yardimci, *Equiripple FIR Filter Design by the FFT Algorithm*, IEEE Signal Processing Magazine, March 1997.

[15] L. D Grossmann and Y. C. Eldar, *An L_1-Method for the Design of Linear-Phase FIR Digital Filters*, IEEE Transaction on Signal Processing, Vol. 55, No. 11, November 2007.

[16] A. Ben-Israel and T. N. E. Greville, *Generalized Inverses: Theory and Applications*, New York: Wiley, 1977.